Asian Journal of Chemistry; Vol. 34, No. 9 (2022), 2325-2330

ASIAN JOURNAL OF CHEMISTRY

https://doi.org/10.14233/ajchem.2022.23833

in vitro Antibiofilm Evaluation of *N-tert*-Butylacrylamide based Hydrogels

K. JAYANTHI[1,2] and P. PAZHANISAMY[3,*]

[1]Research and Development Centre, Bharathiar University, Coimbatore-641046, India
[2]Department of Chemistry, Loganatha Narayanasamy Government College, Ponneri-601204, India
[3]Department of Chemistry, Sir Theagaraya College, Chennai-600021, India

*Corresponding author: E-mail: p_pazhanisamy@yahoo.com

Received: 14 March 2022; *Accepted*: 20 June 2022; *Published online*: 19 August 2022; AJC-20929

By free-radical copolymerization, a series of *N-tert*-butylacrylamide based hydrogels *viz.* poly(*N-tert*-butylacryalmide-*co*-acrylamide/maleic acid) (**HG11**), poly(*N-tert*-butylacryalmide-*co*-acrylamide/*N*-isopropylacrylamide) (**HG23**) and poly(*N-tert*-butylacrylamide-*co*-acrylamide/acrylic acid) (**HG35**) were synthesized. Infrared spectral investigations, SEM, XRD, and TGA were used to characterize the prepared hydrogels. Biofilm quantification for *Staphylococcus aureus* and *Pseudomonas aeruginosa* was assessed *in vitro* using the microtiter plate (MTP) approach. The hydrogels were found to have the least amount of biofilm formation on their surfaces, indicating that they have superior antibiofilm action and thus low fouling. Fluorescence microscopy was used to examine the morphology to supplement the biofilm inhibition. Among the three hydrogels, **HG11** and **HG35** were found to be more effective against *S. aureus* than *P. aeruginosa*. But **HG23** caused more fouling resistant for *P. aeruginosa* than *S. aureus*.

Keywords: *N-tert*-Butylacrylamide, Hydrogels, Antibiofilm, Maleic acid.

INTRODUCTION

The threat for bacterial contamination in implanted devices is crucial, as infections are expected to kill more people than other medical complications. Antibiotics are commonly used to treat these infections, but biofilm formation on implant surfaces may limit the efficiency of these antibiotics because bacteria within the biofilm are protected from the treatment [1]. Persistent infections are associated with up to 80% of pathogens that produce biofilms. Extracellular polysaccharides, proteins and deoxyribonucleic acid (DNA) make up around 90% of the biofilm mass. Extracellular polysaccharides supports cell stability, mediates surface adhesion and acts as a scaffold for the attachment of cells, enzymes and antibiotics. Persistent bacteria that create biofilms include *Pseudomonas aeruginosa*, attribute to the cystic fibrosis [2], while *Staphylococcus aureus* causes the majority of wound infections [3].

Antibacterial coatings are thought to be an excellent method for preventing biofilm formation and as a result, reducing the associated difficulties. Hydrogel can be coated on urinary catheters, central venous catheters [4], contact lenses, joints, dental implants [5,6] and local injection for drug release and wound healing [7]. Moreover, some types of hydrogels also have inherent antimicrobial properties [8,9]. Most of the strategies investigated to prevent bacterial adhesion and subsequent biofilm formation related to surface design can be classified in broad terms as bacterial repelling and bacteria killing surfaces [10]. The bacterial repelling action is based on the preventing biofilm formation, whereas killing approaches are based on bactericidal surfaces that disrupt bacterial cells on contact, resulting in cell death.

Polyacrylamide polymers derived from the acrylamides [11,12], *e.g.* hydroxyethylacrylamide [13,14], (3-methoxypropyl)acrylamide and *N*-isopropylacrylamide have previously been reported as anti-biofouling coating alternatives. Under physiological conditions, polyacrylamide-based polymers are highly stable over long time periods, allowing them to be used in medical devices with extensive functional lifetimes [15,16]. In this work, three novel hydrophilic hydrogels *viz.* poly(*N-tert*-butylacryalmide-*co*-acrylamide/maleic acid) (**HG11**), poly(*N-tert*-butylacryalmide-*co*-acrylamide/*N*-isopropylacrylamide) (**HG23**) and poly(*N-tert*-butylacrylamide-*co*-acryl-

amide/acrylic acid) (**HG35**) were synthesized, characterized and used as suitable antibiofilms. Free radical crosslinking copolymerization [17] was carried out in methanol-water mixture as polymerization solvent, at 60 ºC in the presence of potassium persulfate (KPS) as initiator and *N*,*N*-methylene bisacrylamide (MBA) as crosslinker.

EXPERIMENTAL

Synthesis of *N*-*tert*-butylacrylamide hydrogels: Acrylamide (AM, Merck) was crystallized from acetone-ethanol mixture potassium persulphate (KPS), maleic acid (MA) acrylic acid (Ac), *N*-isopropylacrylamide (NIPAM) were supplied from Aldrich. The crosslinker *N*,*N*′-methylene-bisacrylamide (MBA) and the accelerator *N*,*N*,*N*′,*N*′-tetramethylethylene diamine (TEMED) were used as received. Acrylonitrile was first washed with 5% NaOH solution in water to remove the inhibitor and then with 3% orthophosphoric acid solution in water to remove basic impurities. Then acrylonitrile was washed with double distilled water and dried over anhydrous $CaCl_2$. The acrylonitrile was then distilled in an atmosphere of nitrogen and reduced pressure. It was then collected in a clean dry Amber coloured bottle and kept in the refrigerator at 5 º C.

N-*t*-Butylacrylamide (NBA) was prepared by the reaction of *t*-butyl alcohol with acrylonitrile.

The composition of monomers, initiator (KPS), crosslinker (MBA) are specified in Table-1. In brief, aqueous solution containing NBA (0.5 g), AM (0.5g), MA/NIPAM/Ac (0.5 g), MBA (0.03 g), KPS (0.05 g), TEMED (1 µL) were placed in methanol -water mixture taken in a glass reaction tubes (80 mL), provided with a gas inlet and outlet. After bubbling nitrogen for 15 min, the contents were placed in oil bath at 60 ºC and the polymerization was conducted for 1 day. After the reaction, the hydrogels were cut into pieces 3-4 mm long. The extracted hydrogels were dried in vacuum oven at 50 ºC to constant weight for further use. The representations of the synthesis of hydrogels are given in **Schemes I-III**.

***in vitro* Antibiofilm activity of hydrogels using microtiter plate assay:** By following method of Christensen *et al.* [18], microtiter plate (MTP) assay with 96 well-flat bottom polystyrene titer plates to assess the efficiency of hydrogel in preventing biofilm formation. The optical density (OD) was determined using a microtitre plate reader (Thermo) at 600 nm for different concen-trations

Ethidium bromide/acridine orange (ETBr/AO) staining by fluorescence microscope: In a 24 well culture plate, 5×10^6 cells/mL of *Staphylococcus aureus*/*Pseudomonas aeruginosa* cells were plated on coverslips and fed with IC_{50} concentration of each hydrogel in nutrient broth. For 1 day, the samples were incubated at 37 ºC in a microbiological incubator. After the cells had been incubated, 50 µL of 1 mg/mL acridine orange and ethidium bromide were added and gently mixed. Finally, the plate was centrifuged for 2 min at 800 rpm and analyzed within 1 h, with at least 100 cells viewed using a fluorescence microscope and a fluorescent filter.

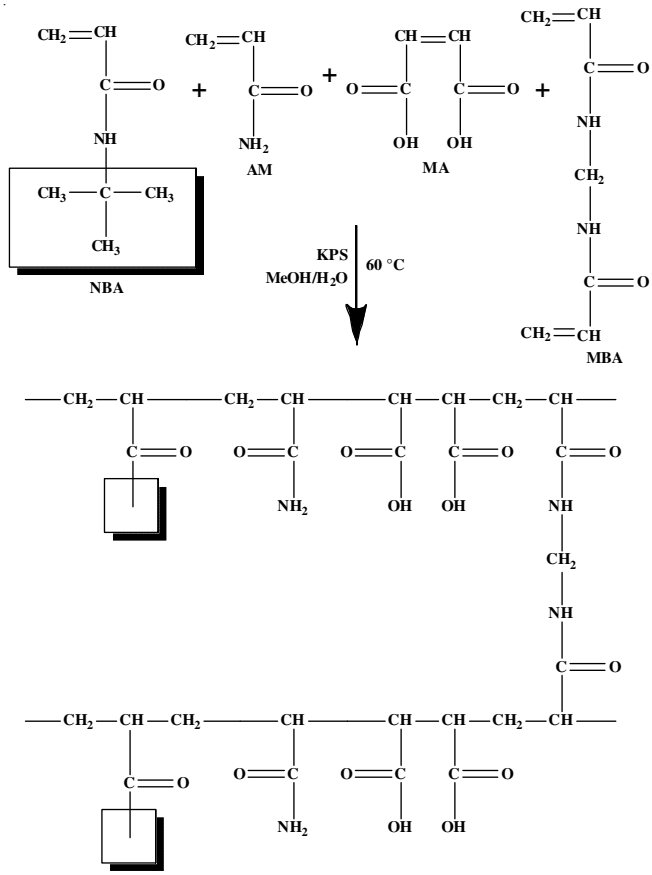

Scheme-I: Poly (NBA-co-AM/MA) hydrogel

RESULTS AND DISCUSSION

FTIR studies: The key FT-IR data of the synthesized hydrogels are given in Table-2. The IR spectra of all hydrogels showed the characteristic absorptions at 3343-3306 cm^{-1} and 1677-1635 cm^{-1} corresponding to the NH stretching and C=O stretching, repectively of NBA, NIPAM and AM.The absorption at 2977-2949 cm^{-1} is due to C-H stretching of polymer backbone. The characteristic band at 1550-1531 cm^{-1} is attributed to N-H bending of AM unit. The bands at 1390-1363 cm^{-1} and 1269-1213 cm^{-1} correspond to *tert*.-butyl group (Fig. 1). The IR spectra of all the hydrogels indicated the presence of all monomeric units in the crosslinked hydrogel.

SEM studies: SEM images (Fig. 2) of three prepared hydrogels clearly depicted the porous structure indicating that the hydrogels can adsorb or retain water.

TABLE-1
COMPOSITION OF MONOMERS FOR THE PREPARATION OF HYDROGELS

Hydrogel	Weight of NBA (g)	Weight of AM (g)	Weight of MA (g)	Weight of NIPAM (g)	Weight of Ac (g)	Weight of KPS (g)	Weight of MBA (g)	Volume of methanol-water mixture
HG11	0.500	0.500	0.500	–	–	0.050	0.03	20
HG23	0.500	0.500	–	0.500	–	0.050	0.03	20
HG35	0.500	0.500	–	–	0.500	0.050	0.03	20

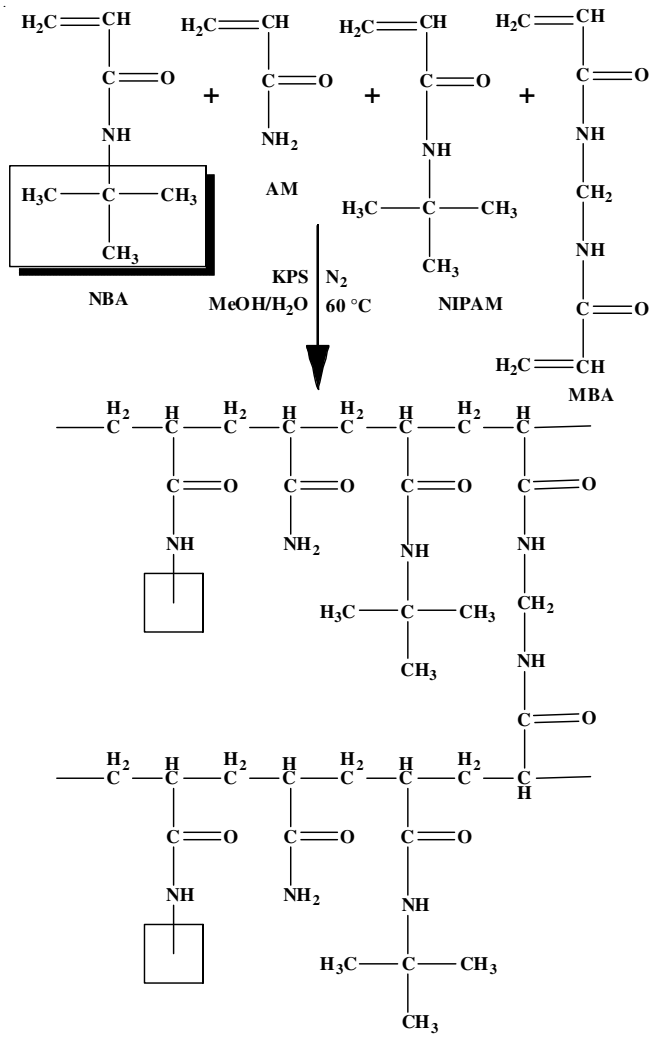

Scheme-II: Poly (NBA-co-MA/NIPAM) hydrogel

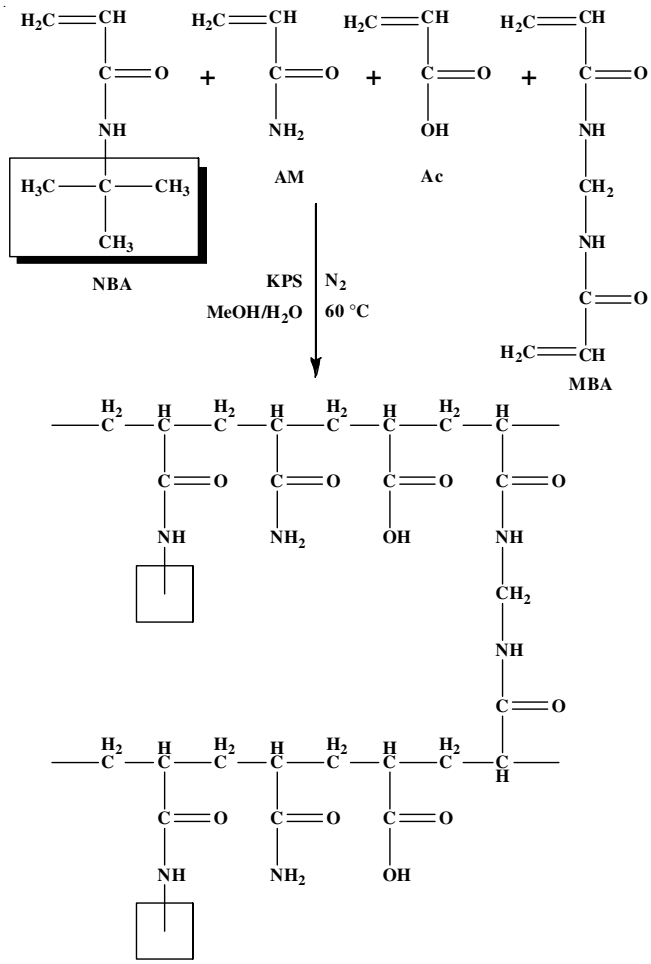

Scheme-III: Poly (NBA-co-MA/Ac) hydrogel

XRD studies: X-ray diffraction patterns of three prepared hydrogels (HG11,HG23 and HG35) show the broadening peak,

TABLE-2
IR ABSORPTION FREQUENCIES AND ASSIGNMENT OF GROUPS

Hydrogel	Absorption frequency (cm^{-1})				
	N-H stretching of NBA and AM	C=O stretching of NBA and AM	C-H stretching of hydrogel backbone	N-H bending of amides (AM)	C-H of tertiary butyl group
Poly(NBA-co-AM/MA) -G11	3343	1677	2977	1531	1363, 1241
Poly(NBA-co-AM/NIPAM-HG23	3306	1635	2977	1550	1363, 1213
Poly(NBA-co-Am/Ac)-HG35	3343	1641	2949	1541	1390, 1269

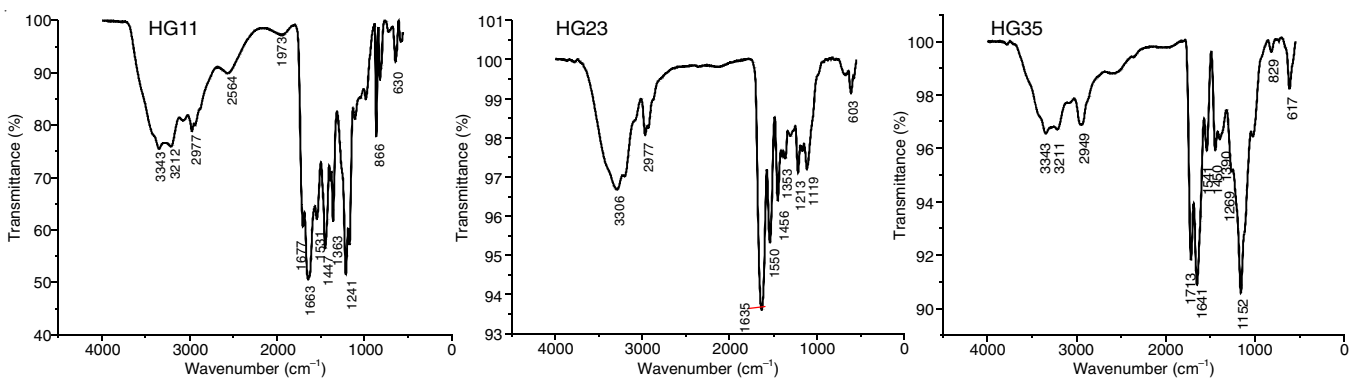

Fig. 1. FTIR spectrum of (a) poly(NBA-co-AM/MA) hydrogel, (b) poly(NBA-co-AM/NIPAM) hydrogel and (c) poly(NBA-co-AM/Ac) hydrogel

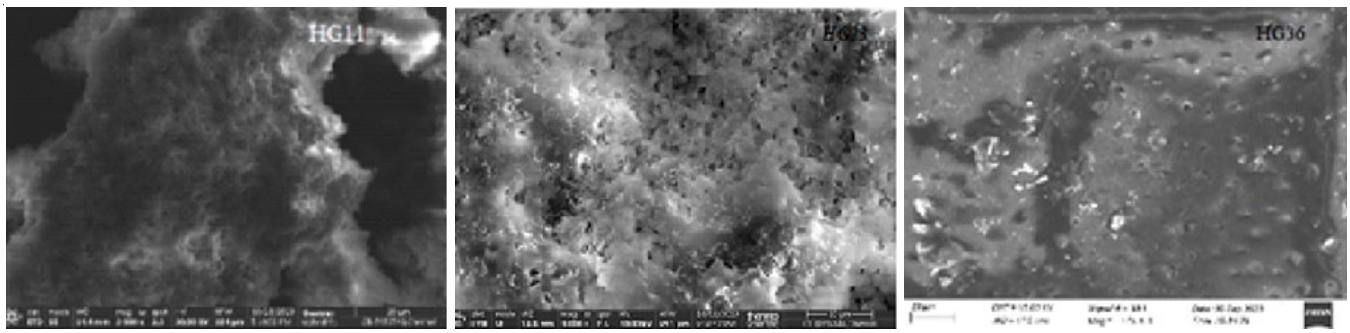

Fig. 2. SEM images of HG11, HG23 and HG35

which conformed the amorphous nature of hydrogels imply its swelling characteristics (Fig. 3).

***in vitro* Antibiofilm screening effect**: In this work, *in vitro* antibiofilm screening effect were studied using the microtiter plate assay. From the OD values of hydrogels, the percentage biofilm inhibition was calculated using the following formula and the values are tabulated in Table-3.

$$\text{Biofilm inhibition (\%)} = \frac{\text{Control OD} - \text{Test OD}}{\text{Control OD}} \times 100$$

The IC_{50} was then calculated using graph pad prism software. The IC_{50} values for HG11 was 21.86 µg/mL against *S. aureus* and 25.57 µg/mL against *P. aeruginosa*, respectively. These values were found to be the least and therefore poly-(NBA -*co*-AM/MA) hydrogels exhibited very good antibiofilm activity. Against *S. aureus* and *P. aureginosa* for poly(NBA -*co*-AM/NIPAM) hydrogels, the IC_{50} values were 34.09 and 29.87µg/mL, respectively. Whereas for poly(NBA-*co*-AM/Ac) hydrogels, the IC_{50} were found to be 29.20 µg/mL against *S. aureus* and 33.66 µg/mL against *P. aureginosa*.

Fluorescent microscopic studies: Fluorescence microscopy is used to investigate the antibiofilm properties of the prepared hydrogels. With acridine orange (AO) nuclear staining, early apoptotic cells appeared as a crescent-shaped or granular yellow-green. Late apoptotic cells were identified by an orange nuclear ethidium bromide (ETBr) staining that was concentrated and asymmetrically located. At the periphery of necrotic cells, there was an irregular orange-red fluorescence with no chromatin fragmentation. Under fluorescent microscopy, the IC_{50} values of hydrogel-treated cells revealed the dead apoptotic bodies (Figs. 4 and 5).

Mechanism of antibiofilm activity: The prepared hydrogels are highly hydrophilic as well as anionic (except HG23).As they are covered with a surface of water molecules, hydrophilic

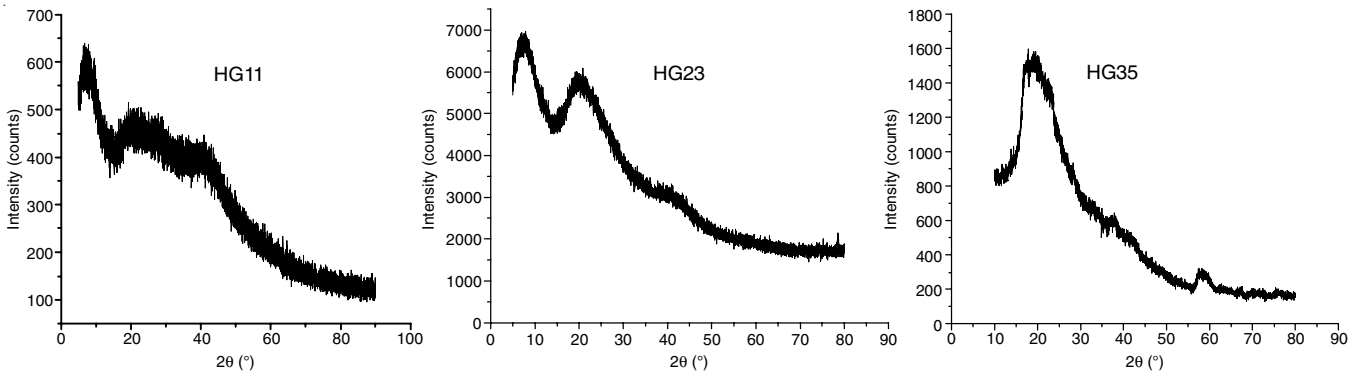

Fig. 3. XRD pattern of HG11, HG23 and HG35

TABLE-3
PERCENTAGE INHIBITION & IC_{50} OF THREE PREPARED HYDROGELS (HG11, HG23 AND HG35)

Conc. (µg/mL)	Biofilm inhibition (%)					
	HG11		HG23		HG35	
	S. aureus	*P. aeruginosa*	*S. aureus*	*P. aeruginosa*	*S. aureus*	*P. aeruginosa*
1	2.17	2.05	1.61	1.62	1.41	2.76
2	2.69	4.26	3.54	4.78	2.90	5.81
4	10.15	10.45	5.29	6.82	7.12	13.99
8	22.71	22.66	110.66	13.24	13.71	16.63
16	27.65	31.19	22.35	24.93	22.08	26.24
32	54.55	49.84	33.26	33.19	51.77	40.31
64	70.16	66.97	40.69	44.71	74.75	67.96
128	76.29	77.36	56.09	49.98	83.08	78.46
256	82.73	88.30	65.95	63.84	92.79	91.78
IC_{50} (µg/mL)	21.86	25.57	34.09	29.87	29.20	33.66

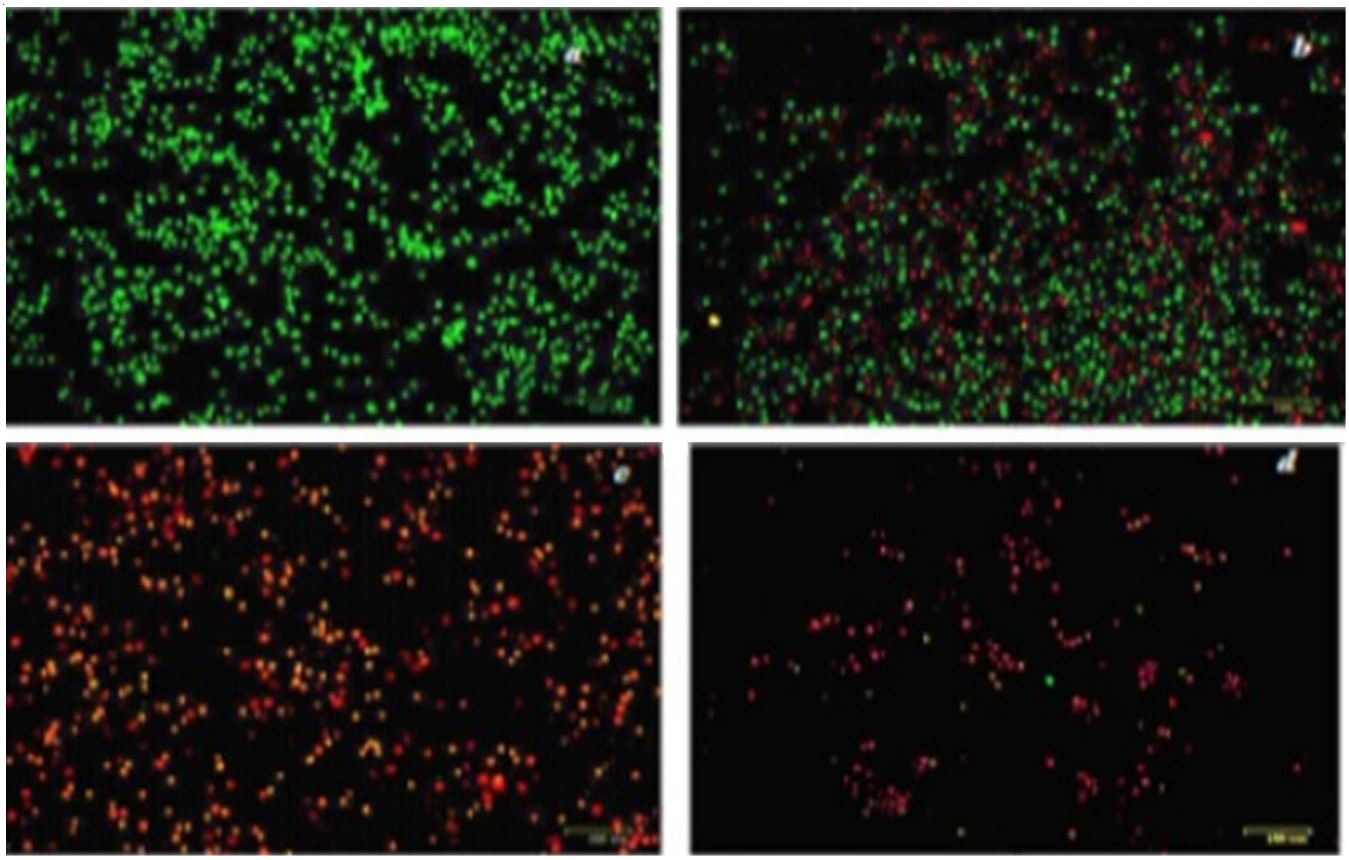

Fig. 4. Fluorescent microscopic images of (a) *S. aureus* (b) Hg11 treated, (c) HG23 treated and (d) HG35 treated

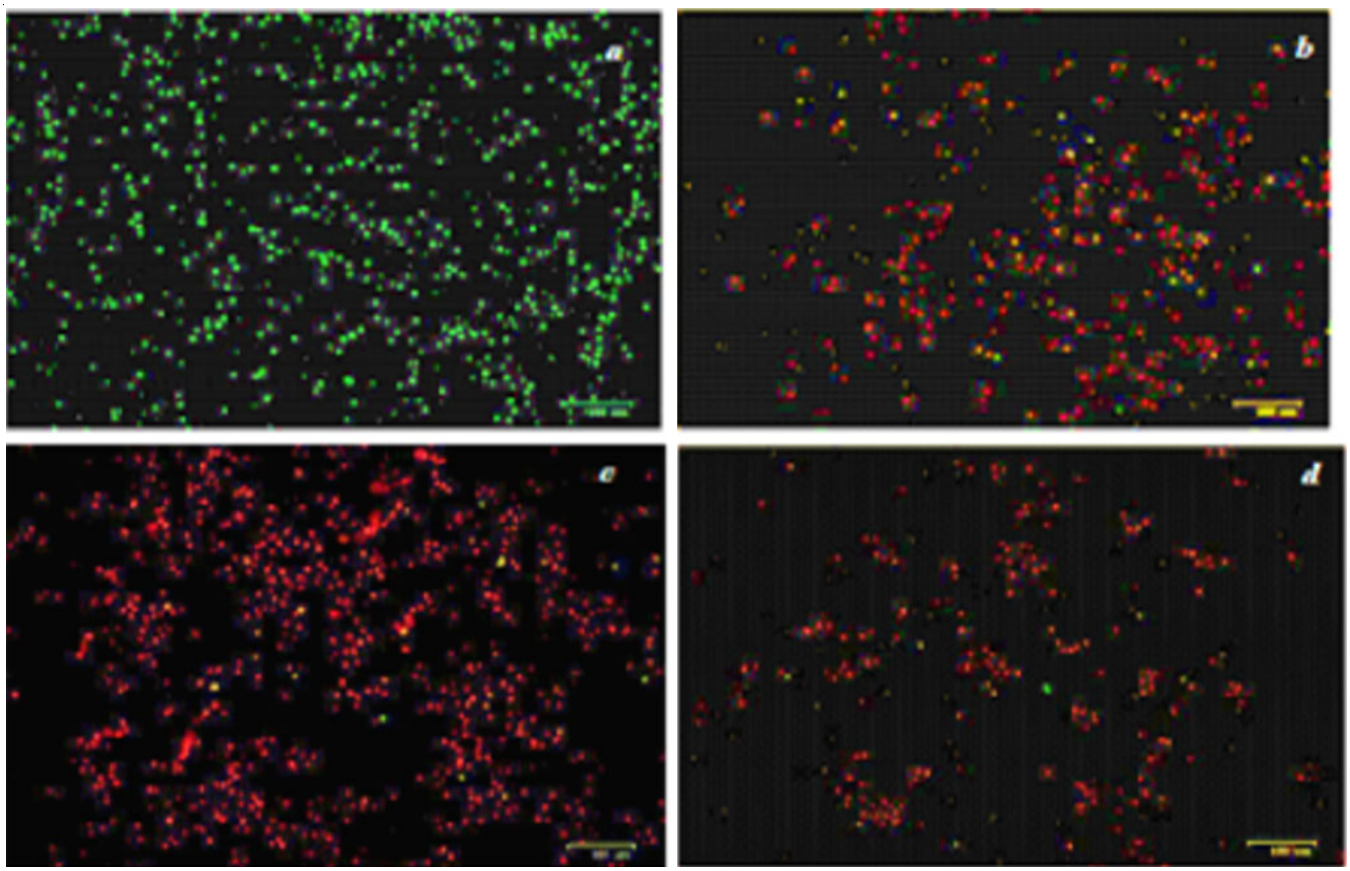

Fig. 5. Fluorescent microscopic images of (a) *P. aeruginosa* (b) Hg11 treated, (c) HG23 treated and (d) HG35 treated

surfaces prevent cells and bacteria from adhering to them and as a result, cells and bacteria cannot be attached. This water layer is tightly bound to the hydrophilic substance by H-bonding, which acts as a physical and energy barrier to cell or bacterial adsorption. It is reported that the irregularities of polymeric surfaces promote bacterial adhesion and biofilm accumulation, whereas the ultra-smooth surface does not prefer bacterial adhesion and biofilm deposition [19]. This is possible because a rough surface has a larger surface area and also the depressions in the roughened surfaces enable better adherence. Kiremitci-Gumustedereliogluand & Pesmen [20] also reported that bacterial adhesion was reduced on the negatively charged PMMA/AA (acrylic acid).

Secondly, the ionization of the carboxyl and phosphate groups gives the bacterial cell surface a negative charge. As a result, when negatively charged surfaces and bacteria cells come close together, electrostatic repulsion occurs, which explains why bacterial adhesion is reduced in general [21]. The structure of adherent bacteria has been found to be affected as a result of strong electrostatic forces [22] and this property compliments to the hydrophilic nature for the effective prevention of bacterial adhesion and hence biofilm formation by both bacteria. Regarding the type of bacteria, IC_{50} values were low for HG11 and Hg35 for *S. aureus* than *P. aeruginosa*, however Hg23 shows higher biofilm inhibition for *P. aeruginosa* than *S. aureus*.

Conclusion

In present study, three prepared hydrophilic hydrogels *viz.* poly(NBA-*co*-AM/MA), poly(NBA-*co*-AM/NIPAM) and poly-(NBA-*co*-AM/Ac) were synthesized by free radical polymerization. All the three hydrogels revealed an admirable inhibitory biofilm activity against the tested bacterial strains *S. aureus* (Gram-positive) and *P. aeruginosa* (Gram-negative) thus the hydrophilic N-*tert*.-butylacrylamide based hydrogels can be found to serve as antibacterial coating on the implant devices,which can prevent the pathogenic infections.

CONFLICT OF INTEREST

The authors declare that there is no conflict of interests regarding the publication of this article.

REFERENCES

1. R. Roy, M. Tiwari, G. Donelli and V. Tiwari, *Virulence*, **9**, 522 (2018); https://doi.org/10.1080/21505594.2017.1313372
2. N. Høiby, O. Ciofu and T. Bjarnsholt, *Future Microbiol.*, **5**, 1663 (2010); https://doi.org/10.2217/fmb.10.125
3. N.K. Archer, M.J. Mazaitis, J.W. Costerton, G. Leid, M.E. Powers and M.E. Shirtliff, *Virulence*, **2**, 445 (2011); https://doi.org/10.4161/viru.2.5.17724
4. S. Noimark, C.W. Dunnill, M. Wilson and I.P. Parkin, *Chem. Soc. Rev.*, **38**, 3435 (2009); https://doi.org/10.1039/b908260c
5. E.M. Hetrick and M.H. Schoenfisch, *Chem. Soc. Rev.*, **35**, 780 (2006); https://doi.org/10.1039/b515219b
6. L.D. Shea, T.K. Woodruff and A. Shikanov, *Annu. Rev. Biomed. Eng.*, **16**, 29 (2014); https://doi.org/10.1146/annurev-bioeng-071813-105131
7. C. Ghobril and M.W. Grinstaff, *Chem. Soc. Rev.*, **44**, 1820 (2015); https://doi.org/10.1039/C4CS00332B
8. N. Sahiner, S. Sagbas, M. Sahiner, C. Silan, N. Aktas and M. Turk, *Int. J. Biol. Macromol.*, **82**, 150 (2016); https://doi.org/10.1016/j.ijbiomac.2015.10.057
9. C.T. Tsao, C.H. Chang, Y.Y. Lin, M.F. Wu, J.-L. Wang, J.L. Han and K.H. Hsieh, *Carbohydr. Res.*, **345**, 1774 (2010); https://doi.org/10.1016/j.carres.2010.06.002
10. K. Vasilev, *Coatings*, **9**, 654 (2019); https://doi.org/10.3390/coatings9100654
11. R. Lalani and L. Liu, *Biomacromolecules*, **13**, 1853 (2012); https://doi.org/10.1021/bm300345e
12. H. Yu, Z. Xu, H. Lei, M. Hu and Q. Yang, *Sep. Purif. Technol.*, **53**, 119 (2007); https://doi.org/10.1016/j.seppur.2006.07.002
13. C. Zhao, X. Li, L. Li, G. Cheng, X. Gong and J. Zheng, *Langmuir*, **29**, 1517 (2013); https://doi.org/10.1021/la304511s
14. C. Zhao, J. Fu, Z. Zhang and E. Xie, *RSC Adv.*, **3**, 4018 (2013); https://doi.org/10.1039/C3RA23182H
15. M.J. Caulfield, G.G. Qiao and D.H. Solomon, *Chem. Rev.*, **102**, 3067 (2002); https://doi.org/10.1021/cr010439p
16. N. Nishiyama, K. Suzuki, H. Yoshida, H. Teshima and K. Nemoto, *Biomaterials*, **25**, 965 (2004); https://doi.org/10.1016/S0142-9612(03)00616-1
17. M. Rizwan, S.R. Gilani, A. Iqbal and D.S. Naseem, *J. Adv. Res*., **33**, 15 (2021); https://doi.org/10.1016/j.jare.2021.03.007
18. G.D. Christensen, W.A. Simpson, J.J. Younger, L.M. Baddour, F.F. Barrett, D.M. Melton and E.H. Beachey, *J. Clin. Microbiol.*, **22**, 996 (1985); https://doi.org/10.1128/jcm.22.6.996-1006.1985
19. T.R. Scheuerman, A.K. Camper and M.A. Hamilton, *J. Colloid Interface Sci.*, **208**, 23 (1998); https://doi.org/10.1006/jcis.1998.5717
20. M. Kiremitci-Gumustedereliogluand A. Pesmen, *Biomaterials*, **17**, 443 (1996); https://doi.org/10.1016/0142-9612(96)89662-1
21. X. Zhang, L. Wang and E. Levänen, *RSC Adv.*, **3**, 12003 (2013); https://doi.org/10.1039/c3ra40497h
22. B. Zdyrko, V. Klep, X. Li, Q. Kang, S. Minko, X. Wen and I. Luzinov, *Mater. Sci. Eng. C*, **29**, 680 (2009); https://doi.org/10.1016/j.msec.2008.12.017